

Fresnel-zone Antennas With Dielectric Phase-Correcting Zones

Lyubomir P. Kamburov¹

Abstract – In this paper we suggest a mathematical model of Fresnel-zones antennas with phase-correcting zones which regards a real thickness of the focusing system. On base of this model is made a numerical analyze of the antennas constructions. The results received with the help of the suggested model are compared with the analyze results of models [1] which examine the focusing system as endless thin.

Keywords – Fresnel antenna, Fresnel-zones, phase-correcting zone, dielectric lenses

I. INTRODUCTION

Fresnel-zones antennas are interesting as an alternatives to the other antennas of optical type, mainly due to easiness of their construction and low production price. Usage of the phase-correcting dielectric rings instead of opaque ones improves aperture synthesis and increase efficiency of such antennas.

The model of dielectric Fresnel-zone antenna is shown in [1]. The focusing system is accepted to be endless thin, transparent and reflection coefficients of the dielectric slab are taken into consideration. In the present paper we suggest a mathematical model of the Fresnel-zones antennas with dielectric phase-correcting zones, which regards a real thickness of the focusing system. The received amplitude-phase distribution of the feed field over the focusing system is also determined following the laws of optical geometry without taking into consideration the influence on the focusing system over this distribution. The numerical analyze of the characteristics of the antennas' systems is performed with aperture method.

II. MATHEMATICAL MODEL

A. Configuration

The configuration of the examined antennas is shown on fig. 1. They consist from the focusing system of dielectric rings (dash lines) with thickness d and the feed situated at the distance F from it. The distribution of the electromagnetic field in the aperture is shown in local spherical coordinates (ρ, ψ, ξ) . A point from the far zone is described with spherical coordinates r, θ and φ .

On fig. 2 is shown a section of antenna's construction in plate XOZ.

¹Lyubomir P. Kamburov is with Department of Radio Engineering, Faculty of Elektronik, Technical University of Varna, Studentska Street 1, Varna 9010, Bulgaria, E-mail: lkambourov@hotmail.com

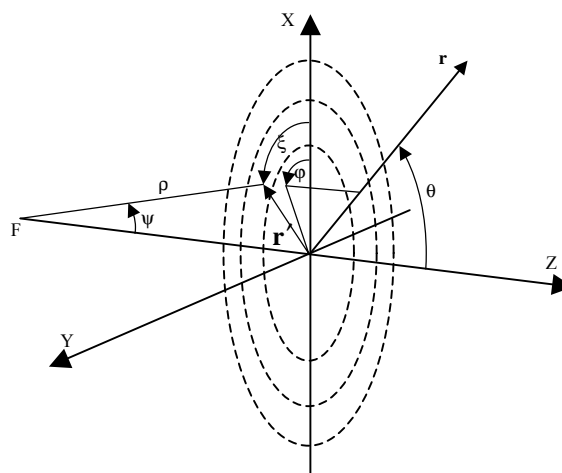


Fig. 1

The radii of the Fresnel zones are calculated as for antennas with transparent/opaque zones and endless thin focusing system with formula [2]:

$$b_m = \sqrt{m\lambda \left(F + \frac{m\lambda}{4} \right)}, \quad (1)$$

where: m is a Fresnel zone number; λ - wave length, F - focusing distance.

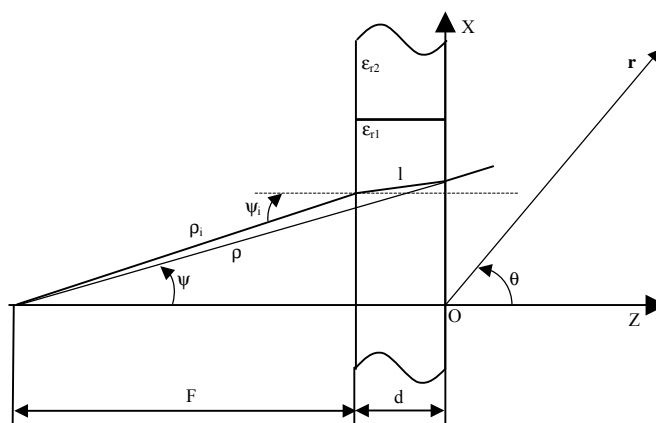


Fig. 2

The thickness of the dielectric rings is chosen identical for even and odd zones and is determined by the requirement for gaining of an additional phase difference between two neighboring zones of 180° . The main advantage of the lenses with identical thickness of even and odd zones is that they are flat from both sides, they do not hold dust, water or snow,

which can change their focussing properties. Beside this they have weaker electric-magnetic shadowing from the dielectric rings edges. At the chosen dielectric permittivity on even and odd zones their thickness is determined with the following formula [1]:

$$d = \frac{\lambda}{2(\sqrt{\epsilon_{r2}} - \sqrt{\epsilon_{r1}})}, \quad (2)$$

where: ϵ_{r1} is relative dielectric permittivity of the first and odd zones, ϵ_{r2} is the relative dielectric permittivity of the even zones. Usually it is accepted that odd zones are open or have permittivity less than even zones permittivity, as the illumination level caused by feed is maximal in the first zone, situated at the center of the focusing system.

As it is shown in [4], for the chosen relative dielectric permittivity ϵ_{r1} , is better the thickness of the add zones to be a whole number of a half wave-length in them when they are transparent for electromagnetic waves. In this case the relative dielectric permittivity of the even zone is determined by the condition:

$$\epsilon_{r2} = \epsilon_{r1} \cdot \left(\frac{n+1}{n}\right)^2, \quad (3)$$

where with n is marked a number of half-waves in odd zones. It is proved that in this case even zones also are containing whole number of half-waves and the focusing system obtain optimal transmitting qualities.

For the point from the illuminating surface with coordinates ρ , ψ , ξ the ray falling angle to the inner surface of the focusing system that reaches it is ψ_i . The transparence angel is ψ_t .

The connection between the falling and transparence angle is determined by Snelius law [3]

$$\frac{\sin(\psi_i)}{\sin(\psi_t)} = \sqrt{\epsilon_r}, \quad (4)$$

where $\epsilon_r = \epsilon_r(1 - j \tan(\delta))$, δ is an angle of dielectric losses.

From geometrical reasons following fig. 2 the connection between ψ and ψ_i is determined by an expression:

$$F \tan(\psi_i) + d \tan(\psi_t) = (F + d) \tan(\psi) \quad (5)$$

B. Gain function of the feed

The gain function of the feed is given by

$$G_f(\psi_i) = \begin{cases} 2(n+1) \cos^n(\psi_i) & 0 \leq \psi_i \leq \frac{\pi}{2} \\ 0 & \psi_i > \frac{\pi}{2} \end{cases}, \quad (6)$$

where n is specified depending on the radiation level in at the aperture end relating to the level in the center. Polarisation of the electric field of the feed is presented by unit vector $\mathbf{e}_f(\psi_i, \xi)$, characterizing the Huygens-source

$$\mathbf{e}_f(\psi_i, \xi) = -\cos(\xi) \cdot \mathbf{e}_{\psi_i} + \sin(\xi) \cdot \mathbf{e}_{\xi} \quad (7)$$

For the dielectric zones, the field polarization vector describing the incident field, is assumed to be given by

$$\mathbf{e}'_f(\psi_i, \xi) = -|T_M| \cos(\xi) \cdot \mathbf{e}_{\psi_i} + |T_E| \sin(\xi) \cdot \mathbf{e}_{\xi} \quad (8)$$

where T_M and T_E are transmission coefficient through dielectric slab, for parallel and perpendicular polarization respectively.

Taking into consideration repeated raw reflection inside the dielectric slab we determine the transmission coefficient through it by an expression [3]:

$$T_{E,M} = \frac{T_{1E,M} T_{2E,M} e^{-j\gamma_d l}}{1 - R_{2E,M}^2 e^{-j2\gamma_d l}}, \quad (9)$$

where $\gamma_d = \frac{2\pi\sqrt{\epsilon_r}}{\lambda}$ is a incidence coefficient in the dielectric slab. With $T_{1,2E,M}$ and $R_{1,2E,M}$ are marked transparency and reflection coefficients of the electromagnetic field. Index 1 is for transparency through free space and 2 for transparency back.

As [1]:

$$T_{1E,M} T_{2E,M} = 1 - R_{1E,M}^2 \quad (10)$$

$$R_{2E,M} = -R_{1E,M} \quad (11)$$

for transparency coefficient through dielectric slab we get:

$$T_{E,M} = \frac{(1 - R_{1E,M}^2) e^{-j\gamma_d l}}{1 - R_{1E,M}^2 e^{-j2\gamma_d l}} \quad (12)$$

Reflection coefficient for perpendicular and parallel polarization are defined with formulae [3]:

$$R_{1E} = \frac{\sin(\psi_t - \psi_i)}{\sin(\psi_t + \psi_i)} \quad (13)$$

$$R_{1M} = \frac{\tan(\psi_t - \psi_i)}{\tan(\psi_t + \psi_i)} \quad (14)$$

C. Electric field in the aperture

The electric field at the surface of the antenna is:

$$\mathbf{E}(\psi_i, \xi) = \sqrt{G_f(\psi_i)} \frac{e^{-jk(\rho_i + l\sqrt{\epsilon_r})}}{\rho_i + l} \sqrt{\frac{Z_w P_t}{2\pi}} \mathbf{e}'_f(\psi_i, \xi), \quad (15)$$

where: P_t is total power radiated by the feed; k – wave number ($k = 2\pi/\lambda$); Z_w – characteristic wave impedance of vacuum.

According to fig.2

$$l = \frac{d}{\cos(\psi_t)} \quad (16)$$

The distance from the feed to the point from the inner surface of the focusing system ρ_i is calculated with formula:

$$\rho_i = \frac{F}{\cos(\psi_i)} \quad (17)$$

D. Electric field in the far field zone

Electric field in the far field zone derive using the Kirchhoff diffraction integral:

$$\mathbf{E}(\mathbf{r}) = \frac{jke^{-jkr}}{2\pi r} \sqrt{\frac{Z_w P_t}{2\pi}} \mathbf{e}_r \times \iint_S [\mathbf{n} \times \mathbf{e}'_f(\psi_i, \xi)] e^{-jk(\rho_i + l\sqrt{\epsilon_r})} \frac{\sqrt{G_f(\psi_i)}}{\rho_i + l} e^{j\mathbf{k} \cdot \mathbf{r}'} dS, \quad (18)$$

where: r is distance from the antenna to the far field zone; \mathbf{r} and \mathbf{e}_r are correspondingly radius - vector and the unit wave

vector in the direction of observation; \mathbf{r}' - vector to a point on the surface; \mathbf{n} - the unit vector normal to the aperture.

Unit vector normal to the antenna's surface in rectangular coordinates is:

$$\mathbf{n} = \begin{pmatrix} 0 \\ 0 \\ 1 \end{pmatrix} \quad (19)$$

The feed polarization of the feed in rectangular coordinates system x, y, z looks like this:

$$\mathbf{e}'_f = \begin{pmatrix} -|T_M| \cos(\psi_i) \cos^2(\xi) - |T_E| \sin^2(\xi) \\ \sin(\xi) \cos(\xi) [-|T_M| \cos(\psi_i) + |T_E|] \\ |T_M| \sin(\psi_i) \cos(\xi) \end{pmatrix} \quad (20)$$

For the vector product $\mathbf{n} \times \mathbf{e}'_f$ in rectangular coordinates we get:

$$\mathbf{n} \times \mathbf{e}'_f = \begin{pmatrix} \sin(\xi) \cos(\xi) [|T_M| \cos(\psi_i) - |T_E|] \\ -|T_M| \cos(\psi_i) \cos^2(\xi) - |T_E| \sin^2(\xi) \\ 0 \end{pmatrix} \quad (21)$$

The unit vector \mathbf{e}_r that determines the direction to the point from the far zone can be written as:

$$\mathbf{e}_r = \begin{pmatrix} \sin(\theta) \cos(\varphi) \\ \sin(\theta) \sin(\varphi) \\ \cos(\theta) \end{pmatrix} \quad (22)$$

Radius vector \mathbf{r}' to the point of the antenna surface is:

$$\mathbf{r}' = \begin{pmatrix} \rho \sin(\psi) \cos(\xi) \\ \rho \sin(\psi) \sin(\xi) \\ 0 \end{pmatrix} \quad (23)$$

On the fig. 2 ρ is determined by relation:

$$\rho = \frac{F+d}{\cos(\psi)}; \quad (24)$$

Using (24) for \mathbf{r}' yields:

$$\mathbf{r}' = \begin{pmatrix} (F+d) \tan(\psi) \cos(\xi) \\ (F+d) \tan(\psi) \sin(\xi) \\ 0 \end{pmatrix} \quad (25)$$

The surface of elementary element dS of the antenna aperture is:

$$dS = h_\psi h_\xi d\psi d\xi, \quad (26)$$

where h_ψ and h_ξ are Lamé coefficients.

The equation (23) gives ratio between rectangular coordinates (x', y', z') and surface of antenna aperture:

$$x' = (F+d) \alpha \cos(\xi) \quad (27)$$

$$y' = (F+d) \alpha \sin(\xi) \quad (28)$$

$$z' = 0, \quad (29)$$

where:

$$\alpha = \tan(\psi) \quad (30)$$

$$d\alpha = \frac{1}{\cos^2(\psi)} \quad (31)$$

For the Lamé coefficient yields:

$$h_\psi = \frac{F+d}{\cos^2(\psi)} \quad (32)$$

$$h_\xi = (F+d) \tan(\psi) \quad (33)$$

from here:

$$dS = \frac{(F+d)^2 \tan(\psi)}{\cos^2(\psi)} d\psi d\xi \quad (34)$$

It is more convenient to write:

$$\begin{aligned} & \sqrt{G_f(\psi_i)} \frac{1}{\rho_i + l} dS = \\ & \sqrt{G_f(\psi_i)} \frac{(F+d)^2 \tan(\psi)}{\rho_i + l \cos^2(\psi)} d\psi d\xi = O(\psi) d\psi d\xi, \end{aligned} \quad (35)$$

where:

$$O(\psi) = \sqrt{G_f(\psi_i)} \frac{(F+d)^2 \tan(\psi)}{\rho_i + l \cos^2(\psi)} \quad (36)$$

Combining the exponential terms in (18) yields:

$$\begin{aligned} & -jk(\rho_i + l\sqrt{\epsilon_r}) + jk\mathbf{e}_r \cdot \mathbf{r}' = \\ & -jk(\rho_i + l\sqrt{\epsilon_r}) + jk(F+d) \sin(\theta) \tan(\psi) \cos(\varphi - \xi) = \\ & M(\psi) + jN(\theta, \psi) \cos(\varphi - \xi), \end{aligned} \quad (37)$$

where:

$$M(\psi) = -jk(\rho_i + l\sqrt{\epsilon_r}) \quad (38)$$

$$N(\theta, \psi) = k(F+d) \sin(\theta) \tan(\psi) \quad (39)$$

and finally:

$$e^{-jk(\rho_i + l\sqrt{\epsilon_r}) + jk\mathbf{e}_r \cdot \mathbf{r}'} = e^{M(\psi)} e^{jN(\theta, \psi) \cos(\varphi - \xi)} \quad (40)$$

Limits for ξ are independent of the size of the Fresnel zone plate antenna: $0 \leq \xi \leq 2\pi$. For ψ integration, the limits are $\psi_m \leq \psi \leq \psi_{m+1}$, with $m = 0, 2, 4 \dots$. The value of ψ_m can be derived from the relation between:

$$\psi_m = \arctan\left(\frac{b_m}{F+d}\right) \quad (41)$$

Replacing (21), (36), (40) in (18) for the electric field in the far zone yields the expression:

$$\begin{aligned} \mathbf{E}(\mathbf{r}) = \sum_{m=0}^{2,4,\dots} C \mathbf{e}_r \times \int_0^{2\pi} \int_{\psi_m}^{\psi_{m+1}} & \begin{pmatrix} \sin(\xi) \cos(\xi) [|T_M| \cos(\psi) - |T_E|] \\ -|T_M| \cos(\psi) \cos^2(\xi) - |T_E| \sin^2(\xi) \\ 0 \end{pmatrix} \\ & O(\psi) e^{M(\psi)} e^{jN(\theta, \psi) \cos(\varphi - \xi)} d\psi d\xi \end{aligned} \quad (42)$$

where is introduced:

$$C = \frac{jke^{-jkr}}{2\pi r} \sqrt{\frac{Z_w P_t}{2\pi}} \quad (43)$$

After the transformation we reach the expression:

$$\mathbf{E}(\mathbf{r}) = \sum_{m=0}^{2,4,\dots} C(r) \mathbf{e}_r \times \int_{\psi_m}^{\psi_{m+1}} O(\psi) e^{M(\psi)} \begin{pmatrix} \sin(2\varphi)B \\ A - \cos(2\varphi)B \\ 0 \end{pmatrix} d\psi \quad (44)$$

where J_0, J_1, J_2 represent Bessel functions of the first kind and order 0, 1, 2 respectively.

Is introduced:

$$A = (|T_M| \cos(\psi) + |T_E|) J_0(N(\theta, \psi)) \quad (45)$$

$$B = (|T_M| \cos(\psi) - |T_E|) J_2(N(\theta, \psi)) \quad (46)$$

Electric field in the far field zone in spherical coordinates looks like:

$$E_r(\mathbf{r}) = 0 \quad (47)$$

$$E_\theta(\mathbf{r}) = \sum_{m=0}^{2,4,\dots} \pi \cos(\varphi) C \int_{\psi_m}^{\psi_{m+1}} O(\psi) e^{M(\psi)} (-A+B) d\psi \quad (48)$$

$$E_\varphi(\mathbf{r}) = \sum_{m=0}^{2,4,\dots} \pi \cos(\theta) \sin(\varphi) C \int_{\psi_m}^{\psi_{m+1}} O(\psi) e^{M(\psi)} (A+B) d\psi \quad (49)$$

E. Antenna radiation patterns

The antenna systems analysed in this report have the x-component of the electric field as the desired component. The y-component is the cross-polarisation component. The co- and cross-polarisation patterns, $CP(\mathbf{e}_r)$ and $XP(\mathbf{e}_r)$ respectively, are [2]:

$$CP(\mathbf{e}_r) = 10 \log \left[\frac{2\pi r^2}{Z_W P_t} |\cos(\varphi) E_\theta(\mathbf{e}_r) - \sin(\varphi) E_\varphi(\mathbf{e}_r)|^2 \right] \quad (50)$$

$$XP(\mathbf{e}_r) = 10 \log \left[\frac{2\pi r^2}{Z_W P_t} |-\sin(\varphi) E_\theta(\mathbf{e}_r) - \cos(\varphi) E_\varphi(\mathbf{e}_r)|^2 \right] \quad (51)$$

III. NUMERICAL RESULTS

On fig. 3 and fig. 4 are shown the directivity diagrams gained from the numerical results of the antenna construction. With the solid line are shown curves gained with the help of the offered mathematical model, with the dot line according to [1]. The antennas are with 11 zones and focusing distance F 100 cm. The diameter of the focusing system yields 120 cm.

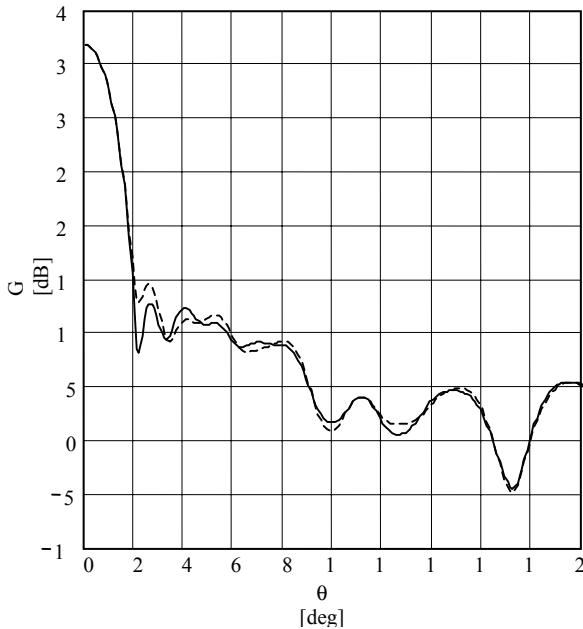


Fig. 3

Diagrams on fig. 3 are for antennas with dielectric permittivity of the odd zones $\epsilon_{r1} = 2.5$, of the even $\epsilon_{r2} = 9$, $\tan \delta = 5 \cdot 10^{-3}$ for the both materials. The thickness of the focusing system in this case yields $d = 1$ cm. On fig. 4 $\epsilon_{r2} = 3.24$ and $d = 5$ cm.

Subsiding relation of the illumination at the end of antenna aperture of the illumination in the center and produced by the feed is -10 dB.

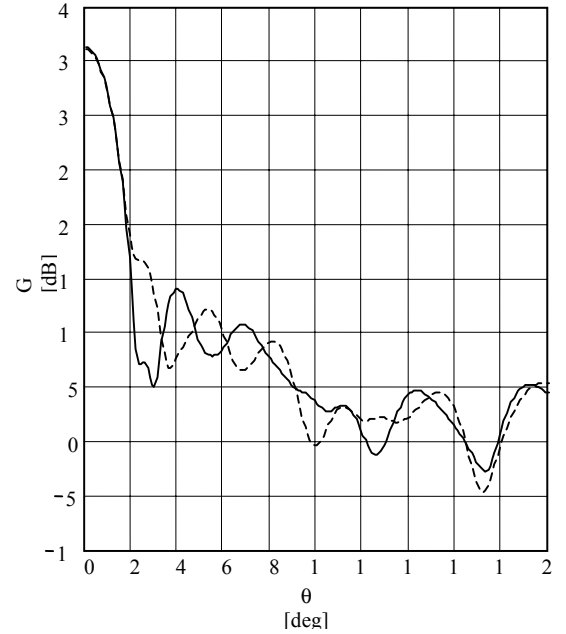


Fig. 4

IV. CONCLUSION

It is obvious, that the directivity diagrams coincide in main lobe as there is difference mainly for side lobes. As expected the difference in diagrams are bigger for the bigger thickness of the focusing system. The accuracy of the model has to be verified during the experimental examination.

REFERENCES

- [1] J. Houten and M. Herben, "Analysis of a phase-correcting Fresnel-zone plate antenna with dielectric/transparent zones", *Journal of Electromagnetic Wave and Applications*, Vol. 4, No. 6, June 1994
- [2] L. Leyten, "Fresnel zone plate antenna versus parabolic reflector antenna", M. Sc. Thesis, Eindhoven University of Technology, Faculty of Electrical Engineering, April 1991
- [3] N. A. Semenov, "Technical Electrodynamics", Svyaz, Moscow, 1973
- [4] L. Kamburov, J. Urumov and H. Hristov, "Fresnel antennas with phase-correcting zones", *International Scientific Conference EIST'01, Conference Proceedings*, vol. 2, pp. 461-466, Bitola, Macedonia, June 7-8, 2001. (in Bulgarian)